Electronic Supplementary Material (ESI) for Journal of Materials Chemistry C.
This journal is © The Royal Society of Chemistry 2018

Impact of the Use of Sterically Congested Cyclometalated Ligands on the Optoelectronic Properties and Device Performances In Light-Emitting Electrochemical Cells of Cationic Iridium(III) Complexes

Claus Hierlinger,[a,b] Elzbieta Trzop,[c] Loïc Toupet,[c] Jorge Ávila,[d] Henk J. Bolink,[d] Véronique Guerchais[a] Eli Zysman-Colman*[b]*

[a] Univ Rennes, CNRS, ISCR (Institut des Sciences Chimiques de Rennes) – UMR 6226, F-35000 Rennes, France. E-mail: veronique.guerchais@univ-rennes1.fr

[b] Organic Semiconductor Centre, EaStCHEM School of Chemistry, University of St Andrews, St Andrews, Fife, KY16 9ST, UK. E-mail: eli.zysman-colman@st-andrews.ac.uk; Web: http://www.zysman-colman.com

[c] Univ Rennes, CNRS, IPR (Institut de Physique de Rennes) - UMR 6251, F-35000 Rennes, France

[d] Instituto de Ciencia Molecular, Universidad de Valencia, C/J. Beltran 2, 46980 Paterna, Spain

SUPPORTING INFORMATION

Table of Contents

Experimental Section 3
Characterization of Compounds 5
Characterization of $[Ir(C^N)_2(dtBubpy)]PF_6$ Complexes 10
X-ray Diffraction Studies 19
LEEC preparation 23

Experimental Section

General Synthetic Procedures

Commercial chemicals were used as supplied. All reactions were performed using standard Schlenk techniques under inert (N_2) atmosphere with reagent-grade solvents. Flash column chromatography was performed using silica gel (Silia-P from Silicycle, 60 Å, 40-63 µm). Analytical thin layer chromatography (TLC) was performed with silica plates with aluminum backings (250 µm with indicator F-254). Compounds were visualized under UV light. ^{1}H, ^{13}C and ^{31}P solution-phase NMR spectra were recorded on a Bruker Avance spectrometer operating at 11.7 T (Larmor frequencies of 500, 400, 126 and 162 MHz, respectively). The following abbreviations have been used for multiplicity assignments: "s" for singlet, "d" for doublet, "t" for triplet and "m" for multiplet. ^{1}H and ^{13}C NMR spectra were referenced to the solvent peak. Melting points (Mps) were recorded using open-ended capillaries on an electrothermal melting point apparatus and are uncorrected. High-resolution mass spectra were recorded at the EPSRC UK National Mass Spectrometry Facility at Swansea University on a quadrupole time-of-flight (ESI-Q-TOF), model ABSciex 5600 Triple TOF in positive electrospray ionization mode and spectra were recorded using sodium formate solution as the calibrant. Elemental analyses were performed by the Service central d'analyse du CNRS at Rennes and by Mr. Stephen Boyer, London Metropolitan University.

Electrochemistry measurements

Cyclic voltammetry (CV) measurements were performed on an Electrochemical Analyzer potentiostat model 600D from CH Instruments. Solutions for cyclic voltammetry were prepared in MeCN and degassed with MeCN-saturated nitrogen bubbling for about 10 min prior to scanning. Tetra(*n*-butyl)ammoniumhexafluorophosphate ($TBAPF_6$; ca. 0.1 M in MeCN) was used as the supporting electrolyte. A Pt wire was used as the pseudoreference electrode; a Pt wire coil was used as the counter electrode and a Pt disk electrode was used for the working

electrode. The redox potentials are reported relative to a saturated calomel electrode (SCE) electrode with a ferrocenium/ferrocene (Fc^+/Fc) redox couple as an internal reference (0.38 V vs SCE).[1]

Photophysical measurements

All samples were prepared in HPLC grade acetonitrile (MeCN) with varying concentrations on the order of μM. Absorption spectra were recorded at RT using a Shimadzu UV-1800 double beam spectrophotometer. Molar absorptivity determination was verified by linear least-squares fit of values obtained from at least three independent solutions at varying concentrations with absorbance ranging from 2.08×10^{-4} to 1.30×10^{-5} M. The sample solutions for the emission spectra were prepared in HPLC grade acetonitrile and degassed via three freeze–pump–thaw cycles. Steady-state luminescence spectra were measured using an Edinburgh FS920 Steady State Fluorimeter combined with a FL920 Fluorescence Lifetime Spectrometer. All samples for steady-state measurements were excited at 400 nm. The spectra were corrected for the wavelength dependence of the detector, and the quoted emission maxima refer to the values after correction. Photoluminescence quantum yields were measured by the optically dilute method[2] using an aerated aqueous solution of $[Ru(bpy)_3]Cl_2$ (Φ_{PL} = 0.042) as the reference.[3] The excitation source for emission lifetime measurements was the 400 nm output (third harmonic) of a Quanta-Ray Q-switched GCR-150-10 pulsed Nd-YAG laser. Luminescence decay signals from a Hamamatsu R928 photomultiplier tube were converted into potential changes by a 50 Ω load resistor and then recorded with a Tektronix Model TDS 620A digital oscilloscope.

Characterization of Compounds

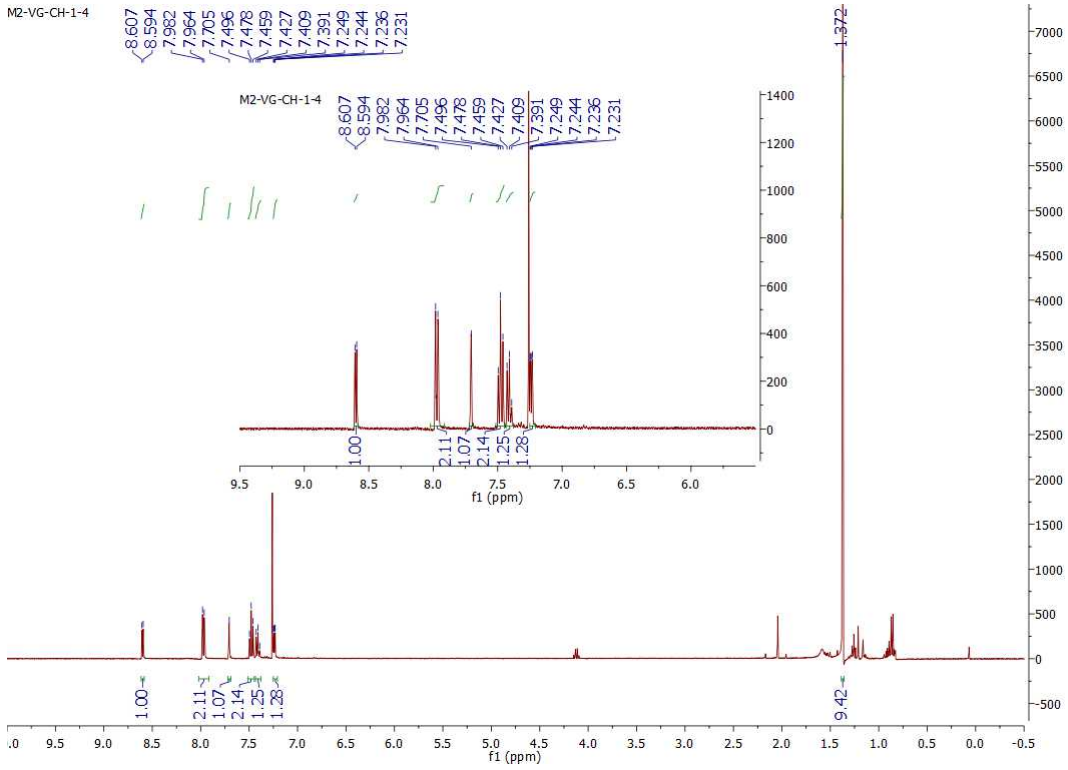

Figure **S1**. ^{1}H NMR spectra of 4-*tert*-butyl-2-phenylpyridine (**L1a**) in $CDCl_3$

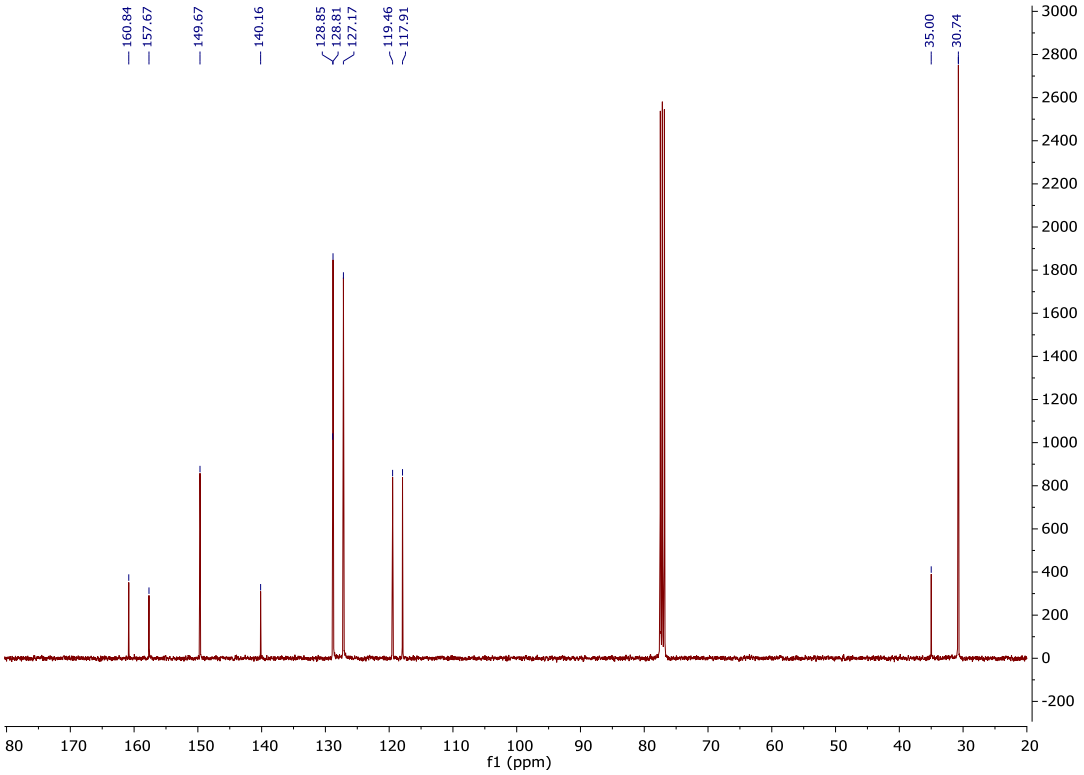

Figure **S2**. ^{31}C NMR spectra of 4-*tert*-butyl-2-phenylpyridine (**L1a**) in $CDCl_3$

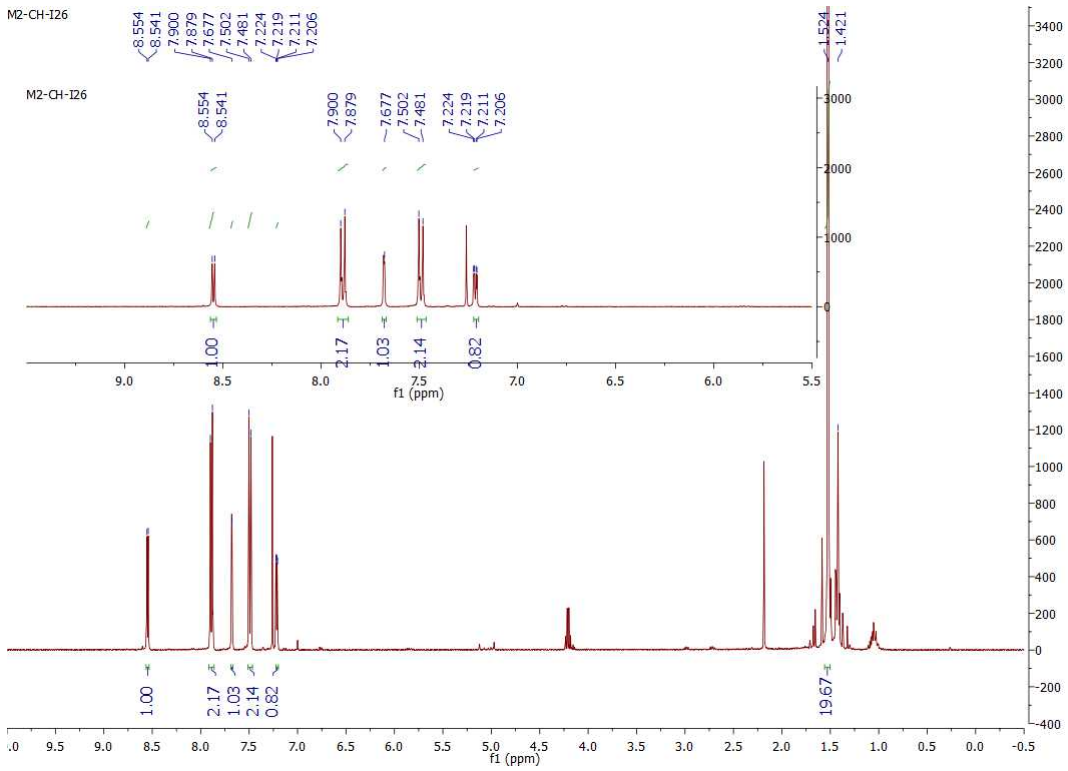

Figure **S3**. ^{1}H NMR spectra of 4-*tert*-butyl-2-(4-*tert*-butylphenyl)pyridine **(L1b)** in $CDCl_3$

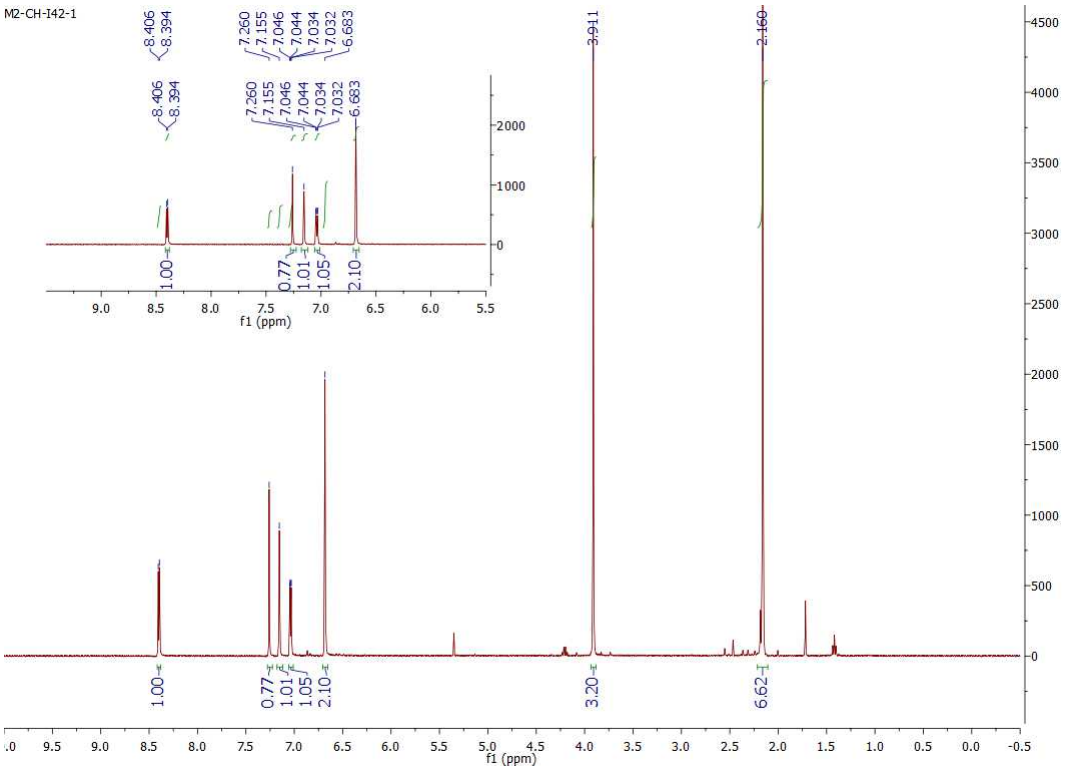

Figure **S4**. ^{1}H NMR spectra of 2-chloro-4-(4-methoxy-2,6-dimethylphenyl)pyridine (**Cl2a**) in $CDCl_3$

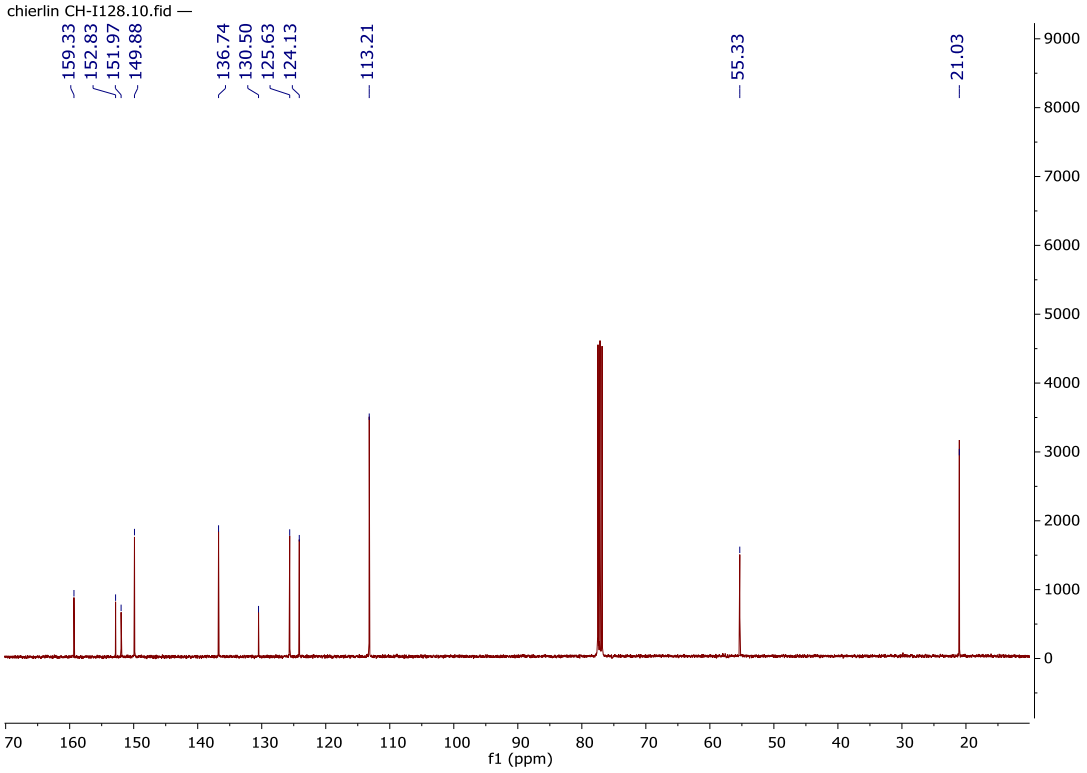

Figure **S5**. ^{13}C NMR spectra of 2-chloro-4-(4-methoxy-2,6-dimethylphenyl)pyridine (**Cl2a**) in $CDCl_3$

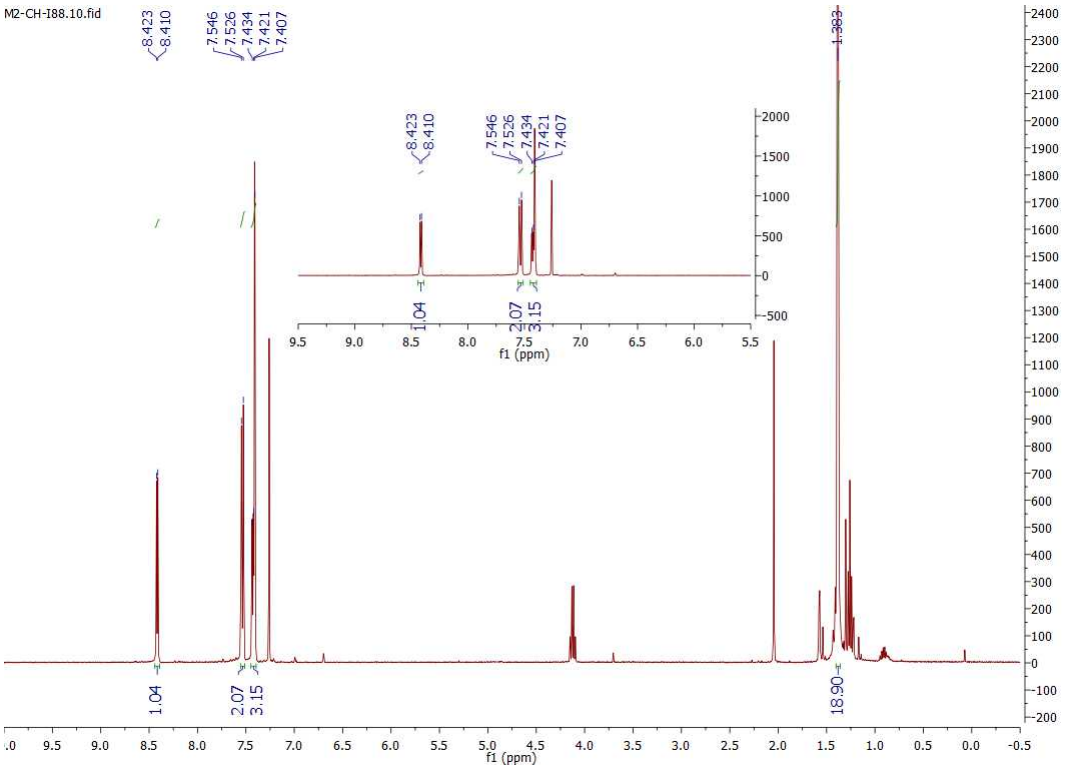

Figure **S6**. ^{1}H NMR spectra of 2-chloro-4-(3,5-di-*tert*-butylphenyl)pyridine (**Cl3a**) in $CDCl_3$

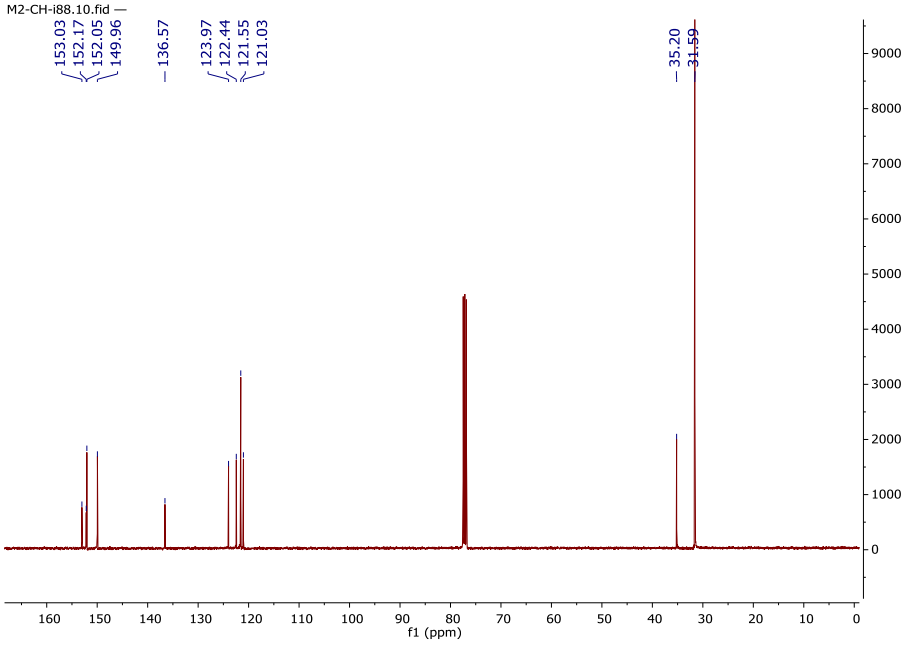

Figure **S7**. ^{13}C NMR spectra of 2-chloro-4-(3,5-di-*tert*-butylphenyl)pyridine (**Cl3a**) in $CDCl_3$

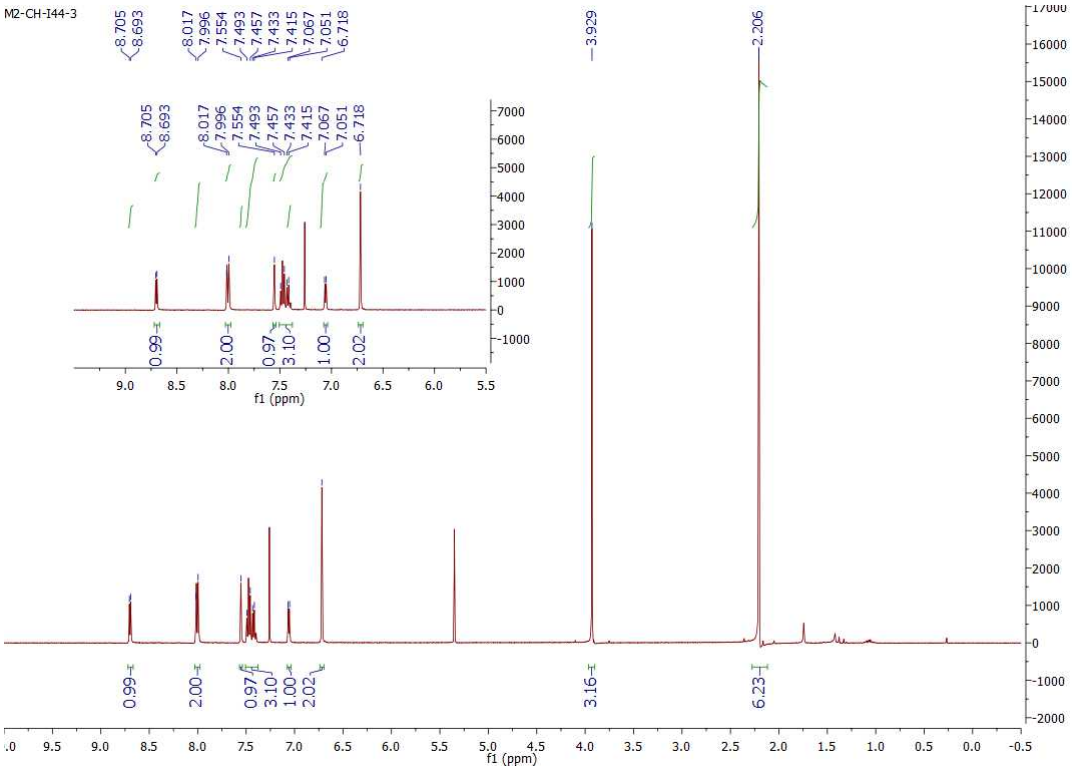

Figure **S8**. ^{1}H NMR spectra of 4-(4-methoxy-2,6-dimethylphenyl)-2-phenylpyridine (**L2a**) in $CDCl_3$

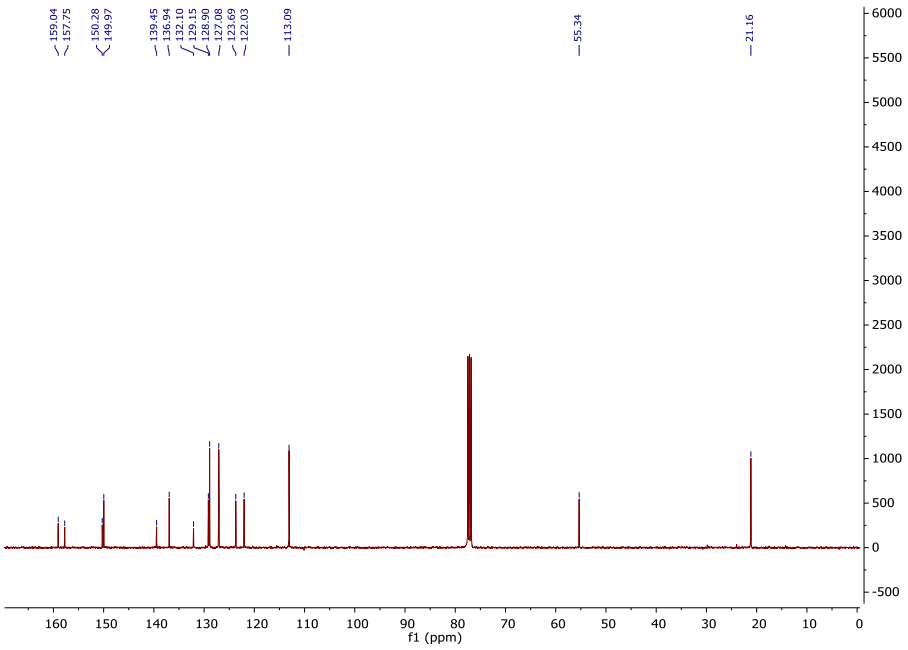

Figure **S9**. ^{13}C NMR spectra of 4-(4-methoxy-2,6-dimethylphenyl)-2-phenylpyridine (**L2a**) in $CDCl_3$

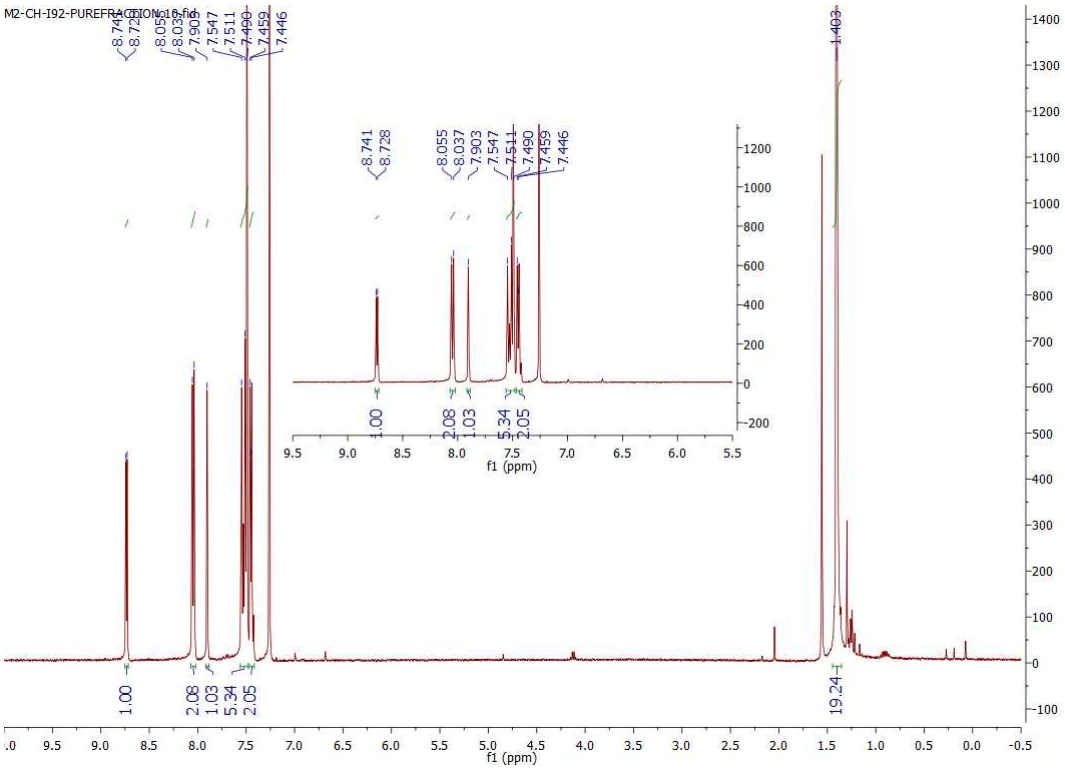

Figure **S10**. ^{1}H NMR spectra of 4-(3,5-di-*tert*-butylphenyl)-2-phenylpyridine (**L3a**) in $CDCl_3$

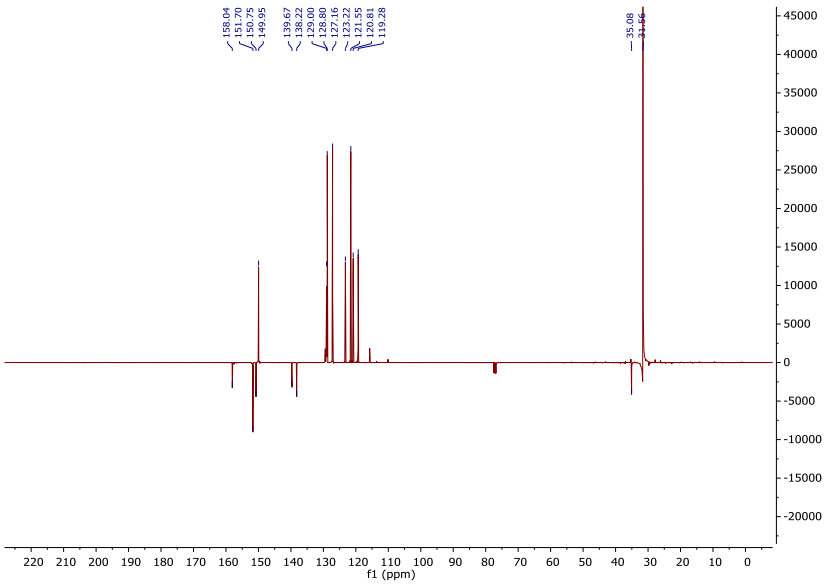

Figure **S11**. ^{13}C NMR spectra of 4-(3,5-di-*tert*-butylphenyl)-2-phenylpyridine (**L3a**) in $CDCl_3$

Characterization of $[Ir(C^{\wedge}N)_2(dtBubpy)]PF_6$ Complexes

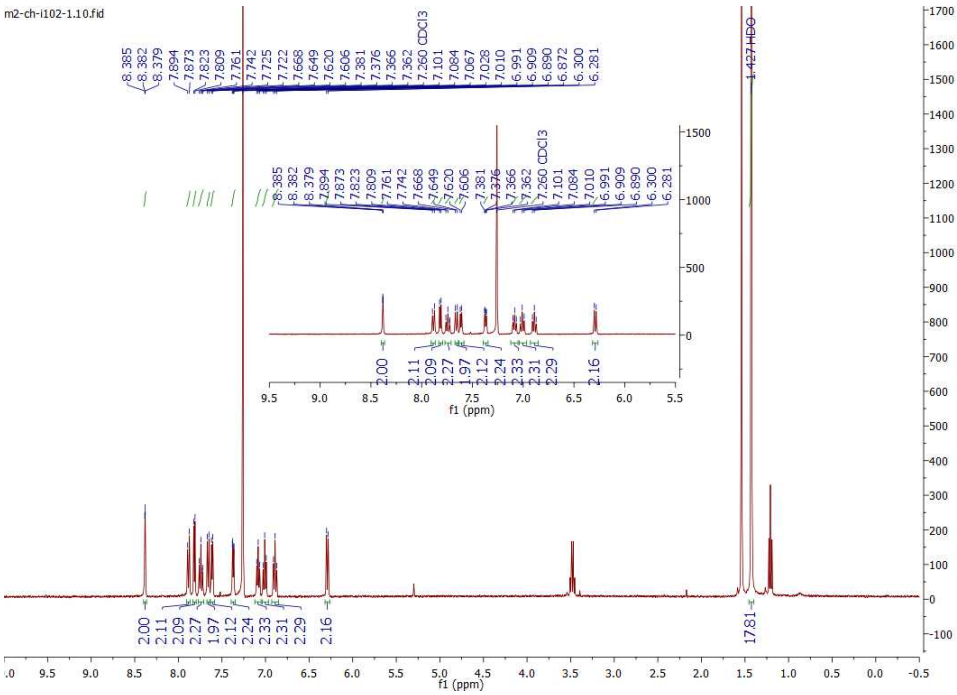

Figure **S12**. ^{1}H NMR spectra of **R1** in $CDCl_3$

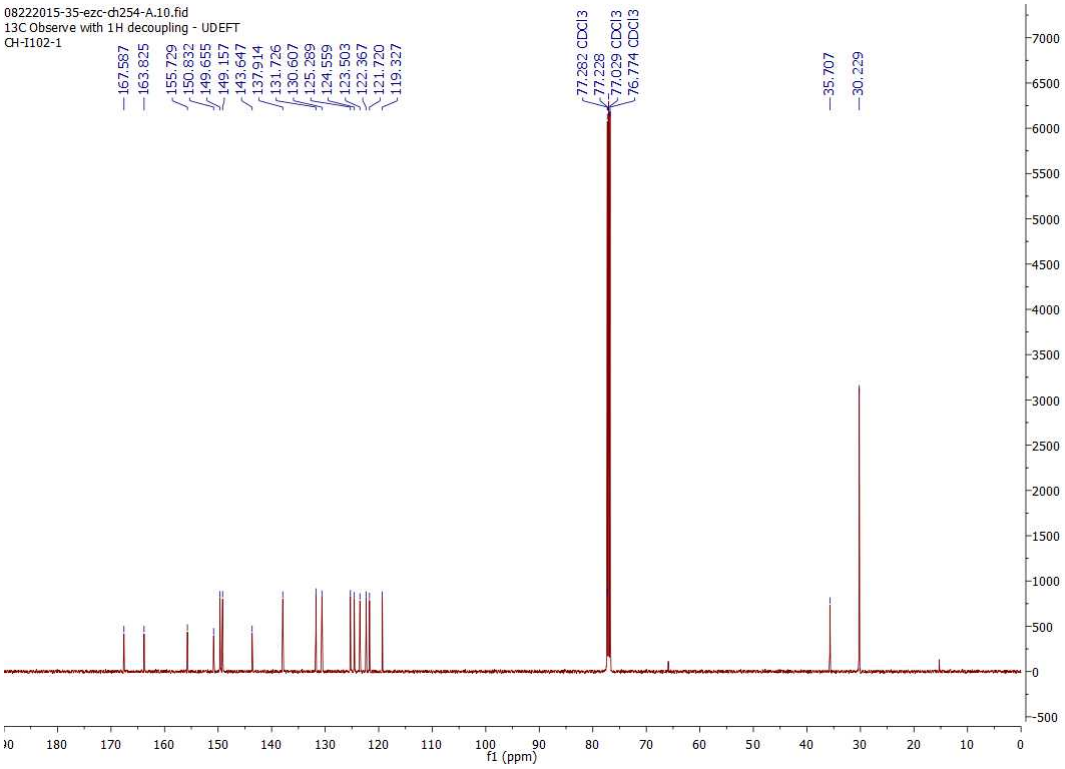

Figure **S8**. ^{13}C NMR spectra of **R1** in $CDCl_3$

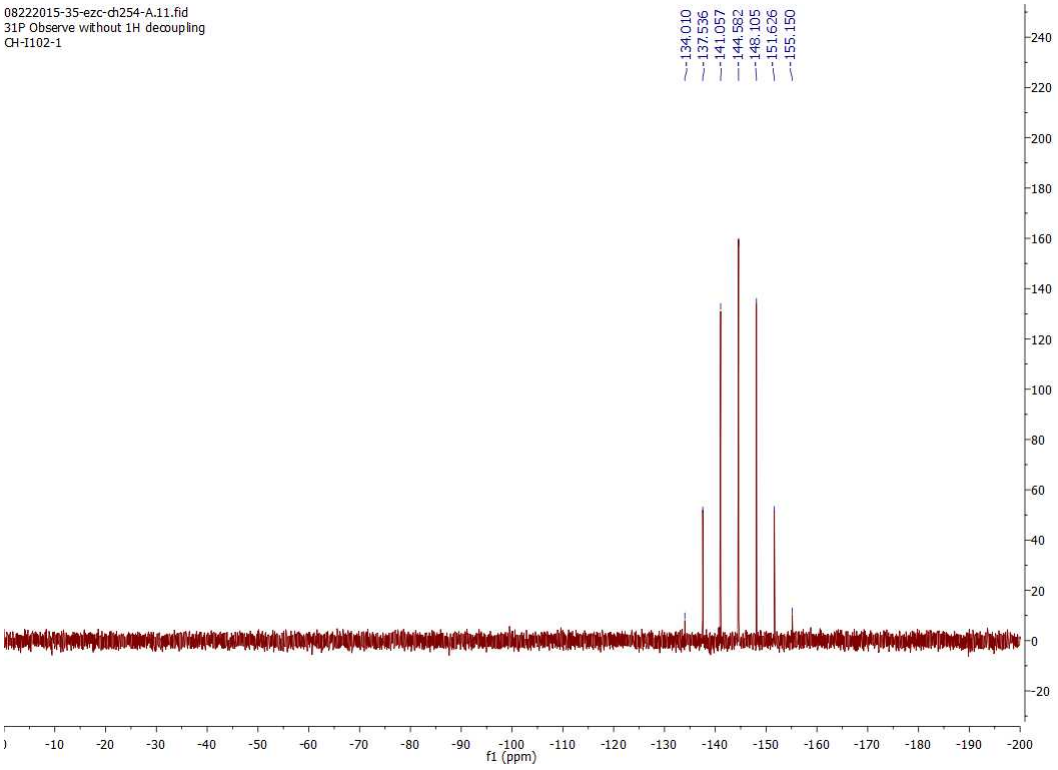

Figure **S9**. ^{31}P NMR spectra **R1** in $CDCl_3$

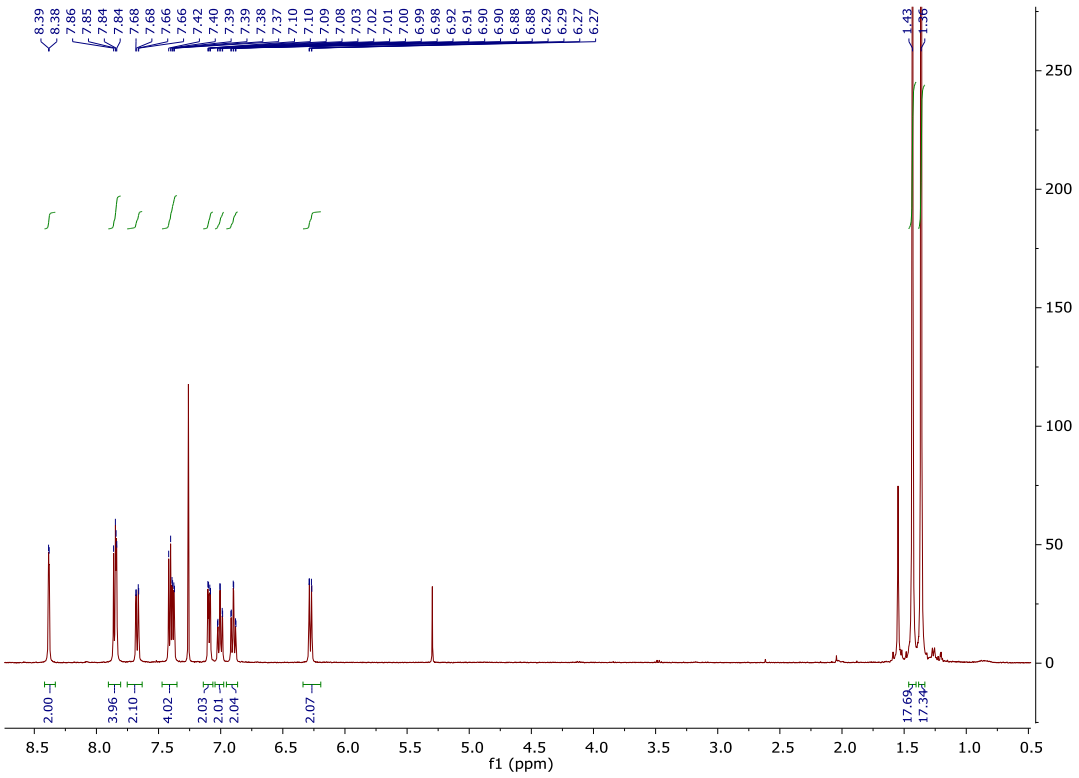

Figure **S10**. ^{1}H NMR spectra of **1a** in $CDCl_3$

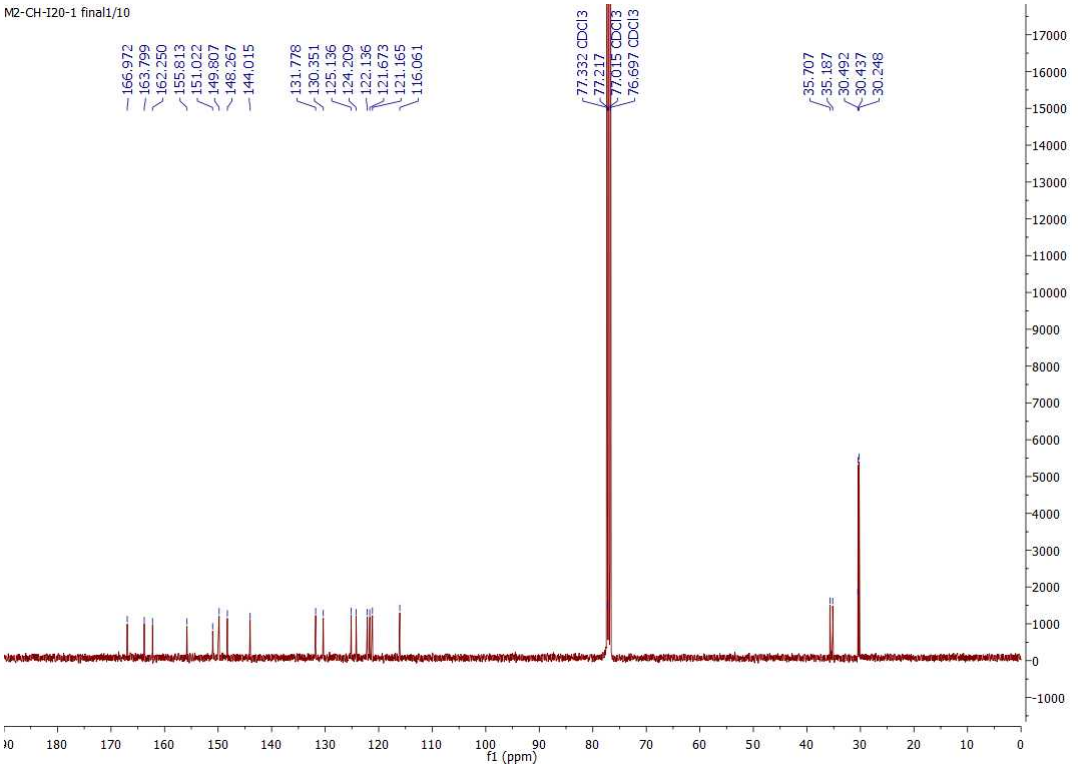

Figure **S11**. ^{13}C NMR spectra **1a** in $CDCl_3$

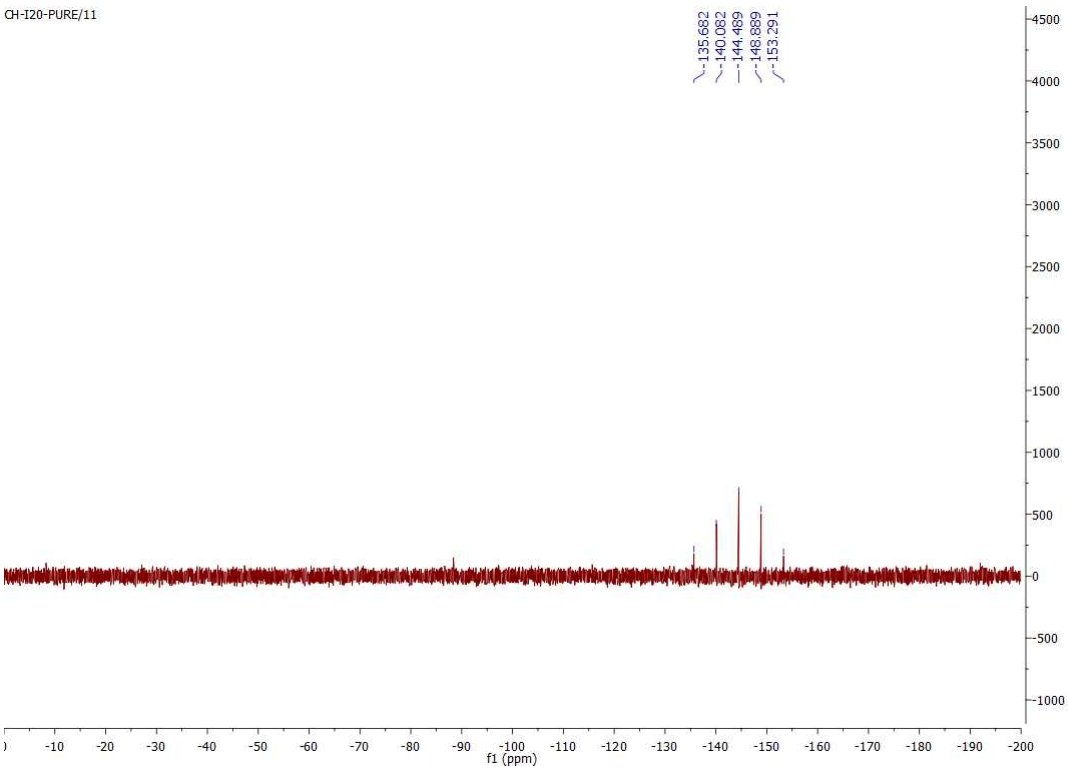

Figure **S12**. ^{31}P NMR spectra of **1a** in $CDCl_3$

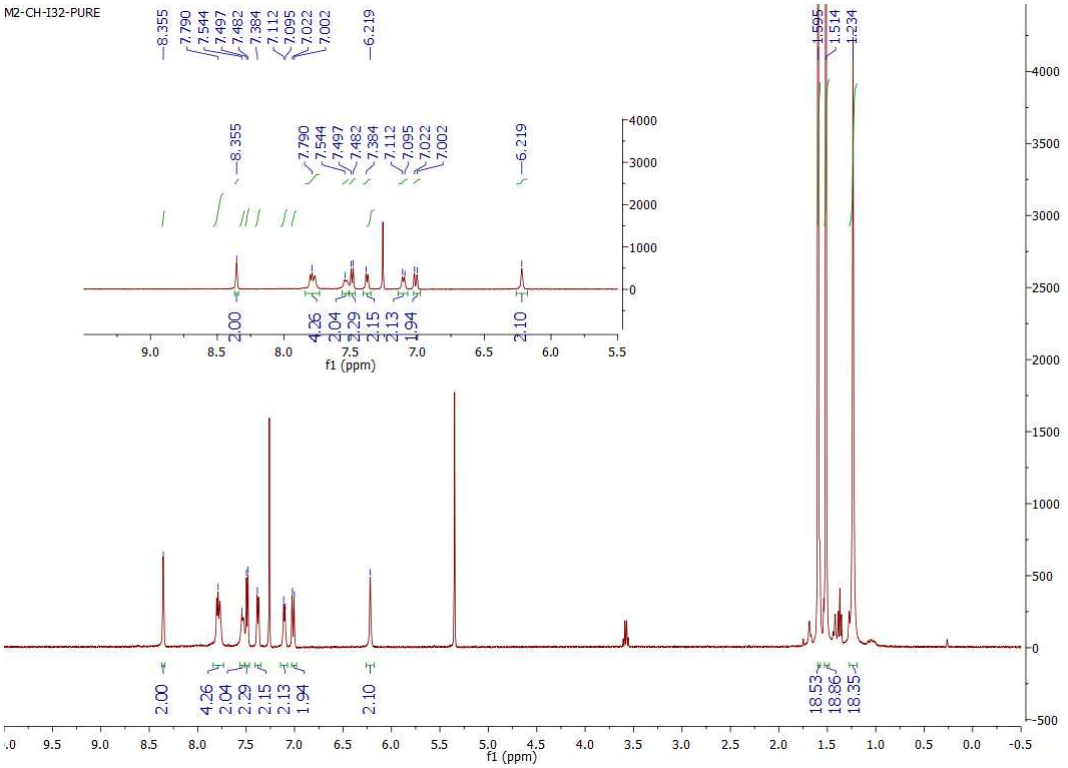

Figure **S13**. ^{1}H NMR spectra of **1b** in $CDCl_3$

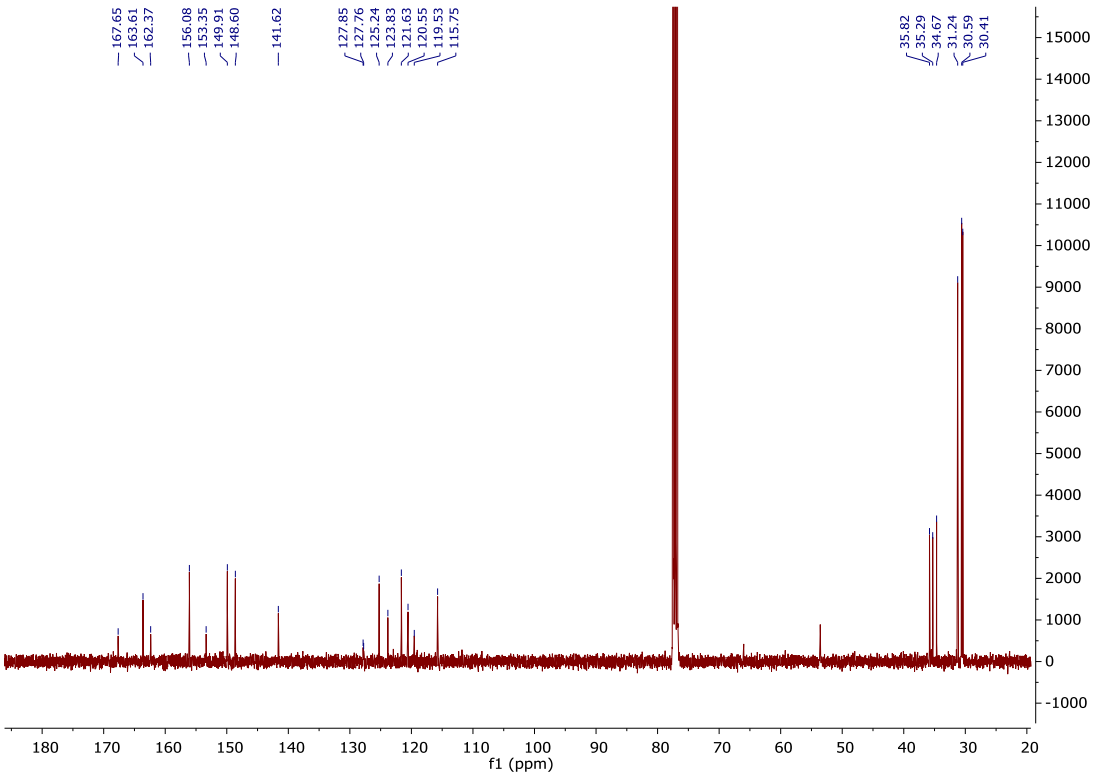

Figure **S14**. ^{13}C NMR spectra of **1b** in $CDCl_3$

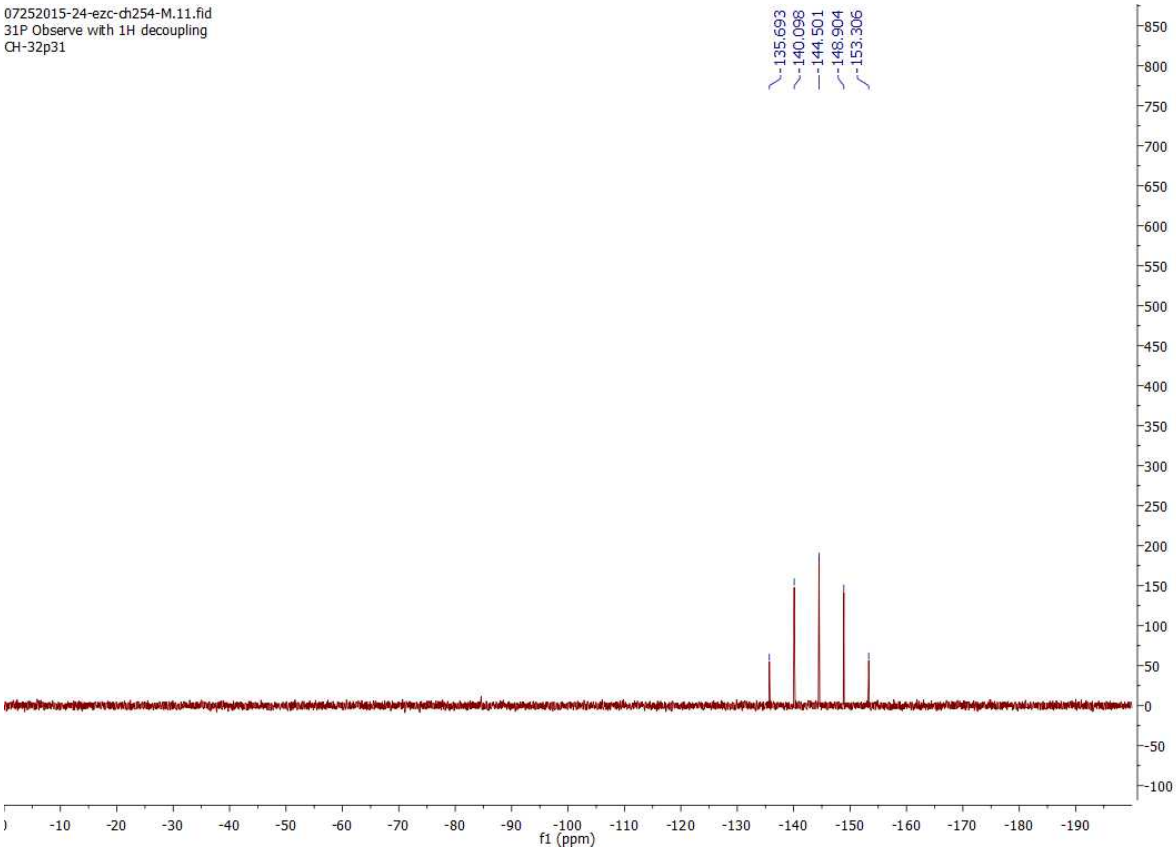

Figure **S15**. ^{31}P NMR spectra of **1b** in $CDCl_3$

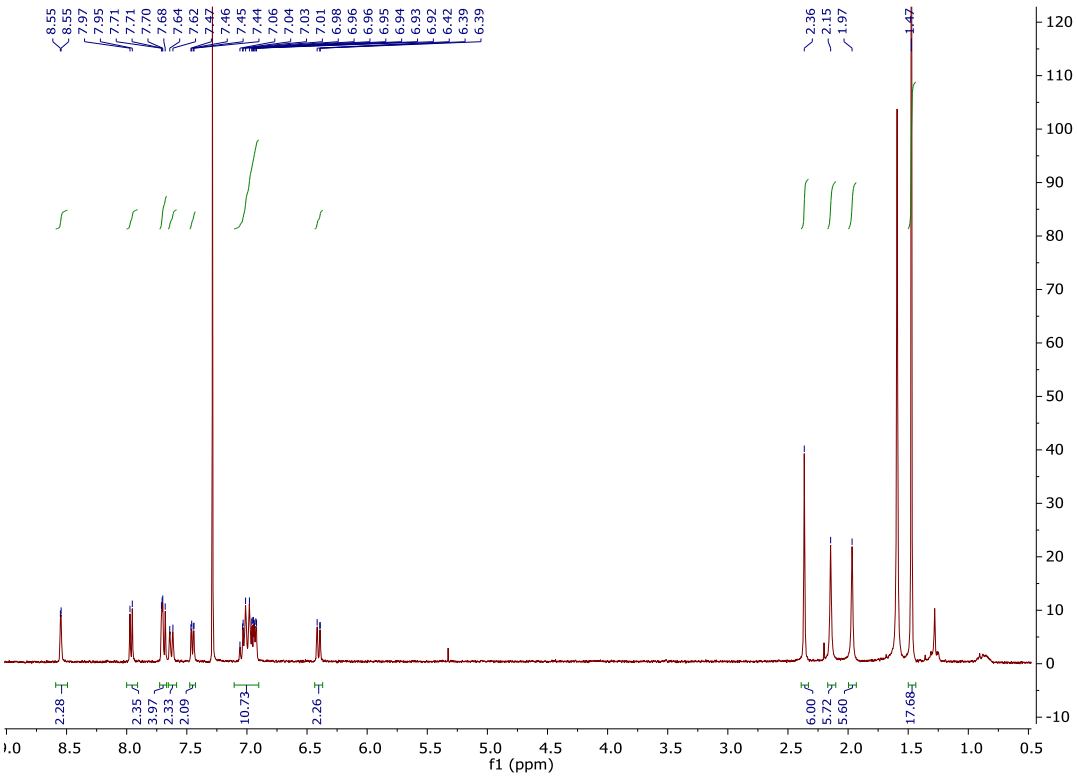

Figure **S16**. ^{1}H NMR spectra of **R2** in $CDCl_3$

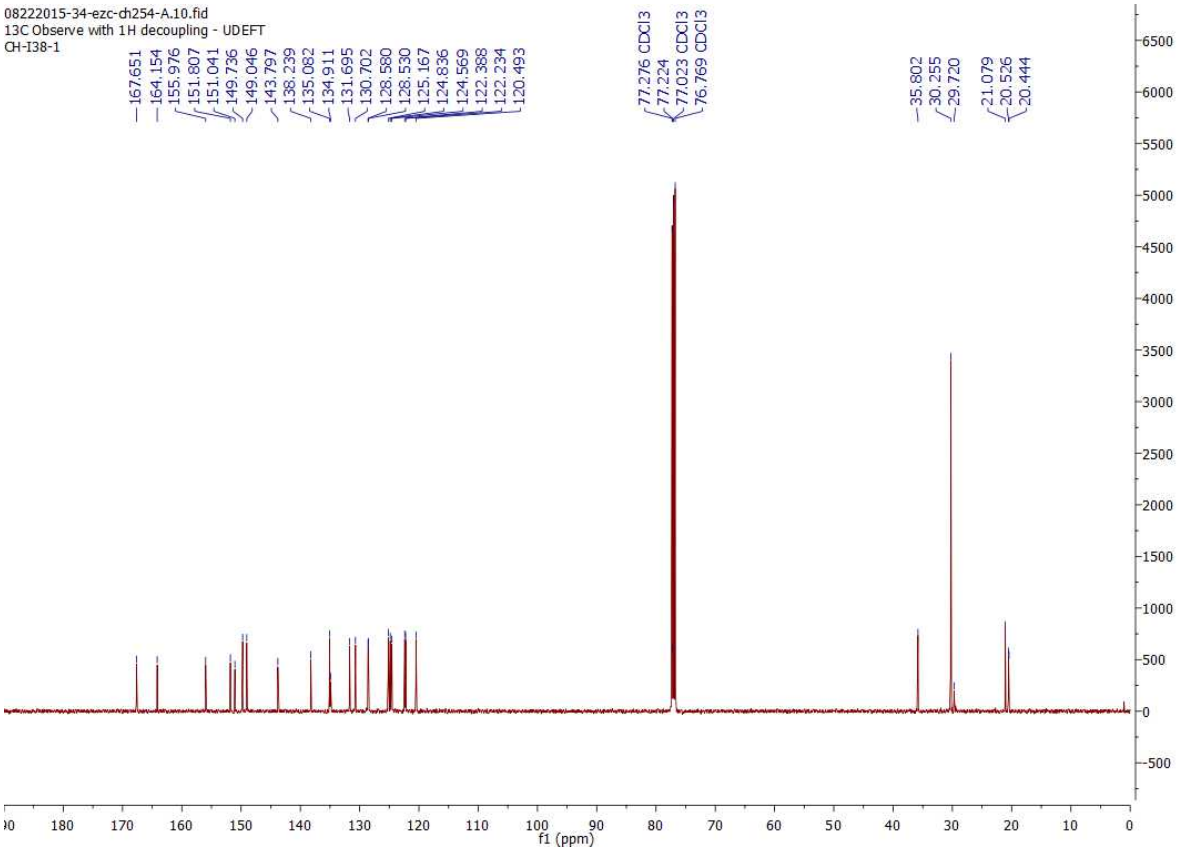

Figure **S17**. ^{13}C NMR **R2** in $CDCl_3$

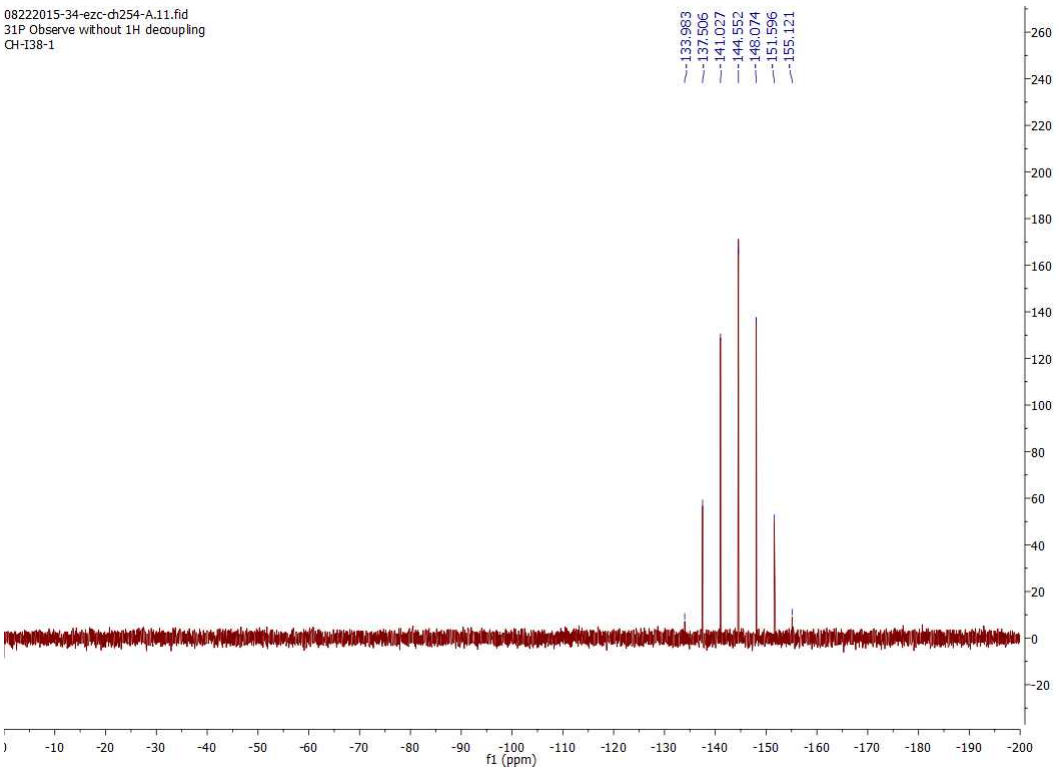

Figure **S18**. ^{31}P NMR spectra of **R2** in $CDCl_3$

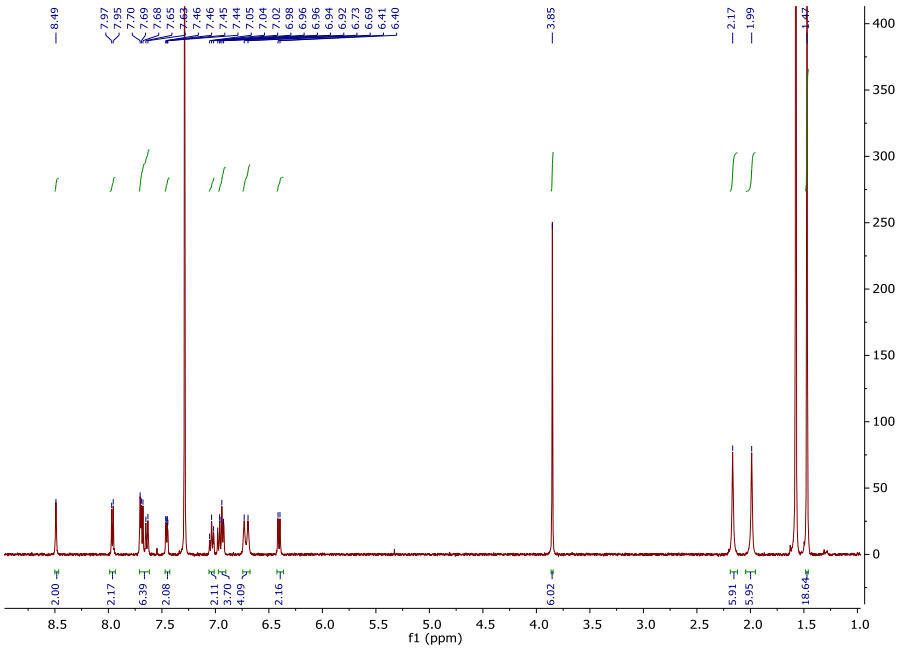

Figure **S19**. ^{1}H NMR spectra of **2a** in $CDCl_3$

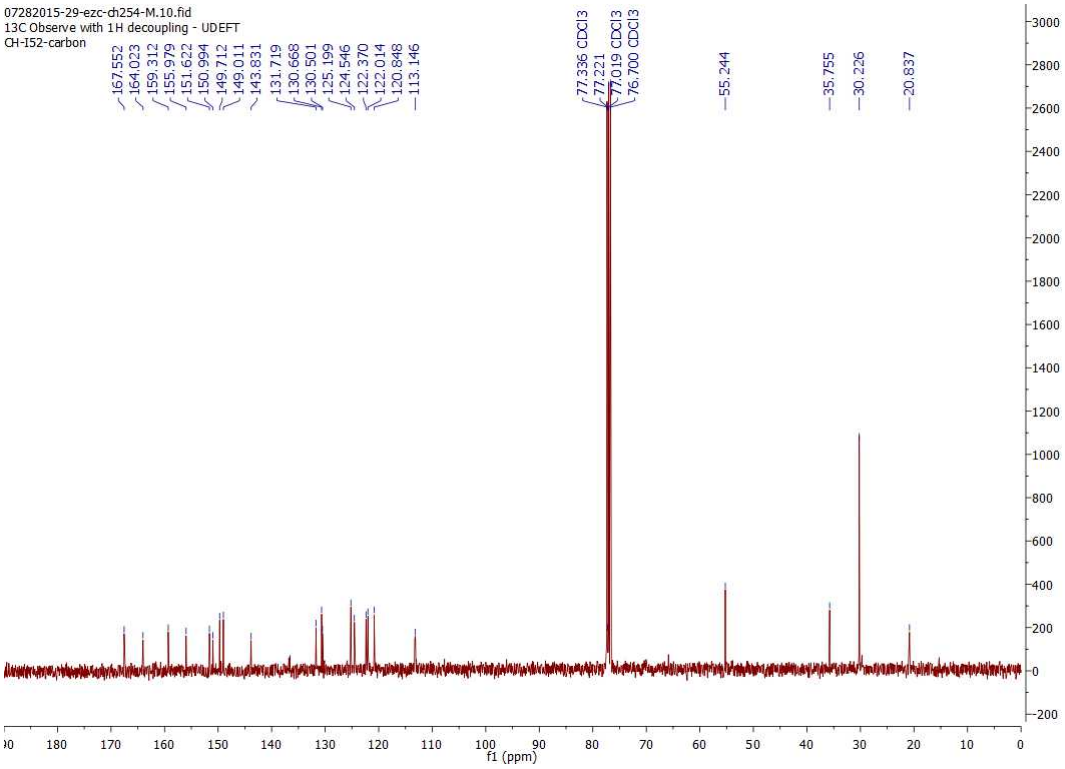

Figure **S20**. ^{13}C NMR spectra of **2a** in $CDCl_3$

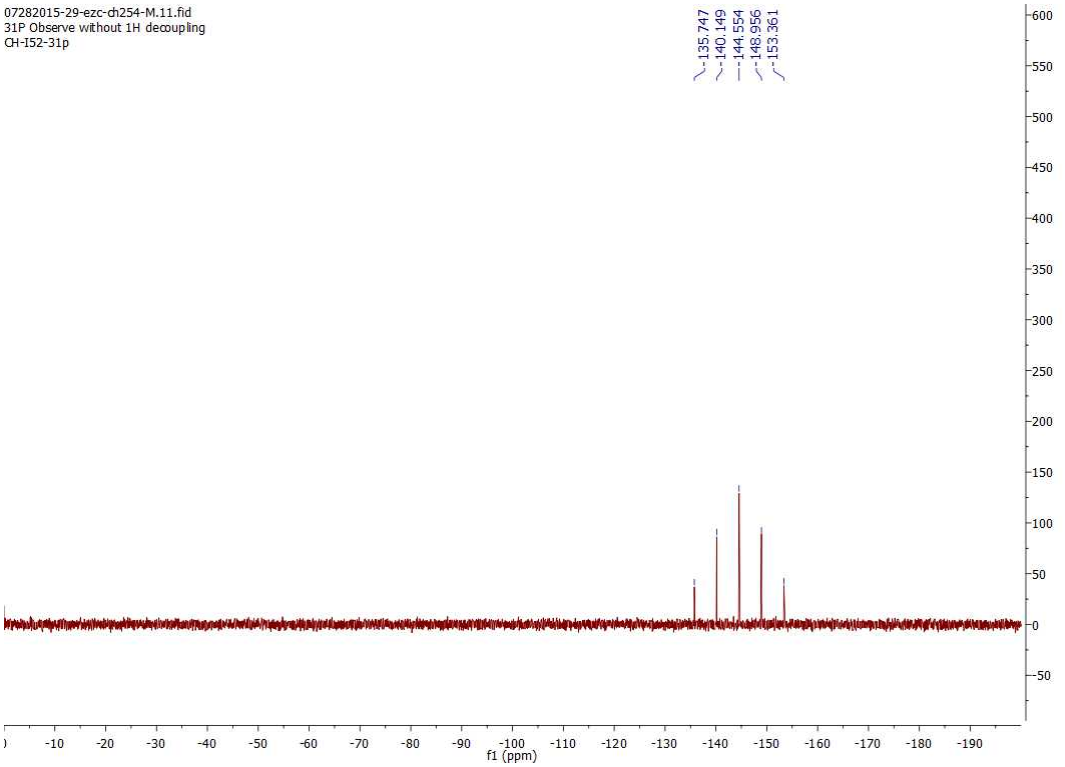

Figure **S21**. ^{31}P NMR spectra of **2a** in $CDCl_3$

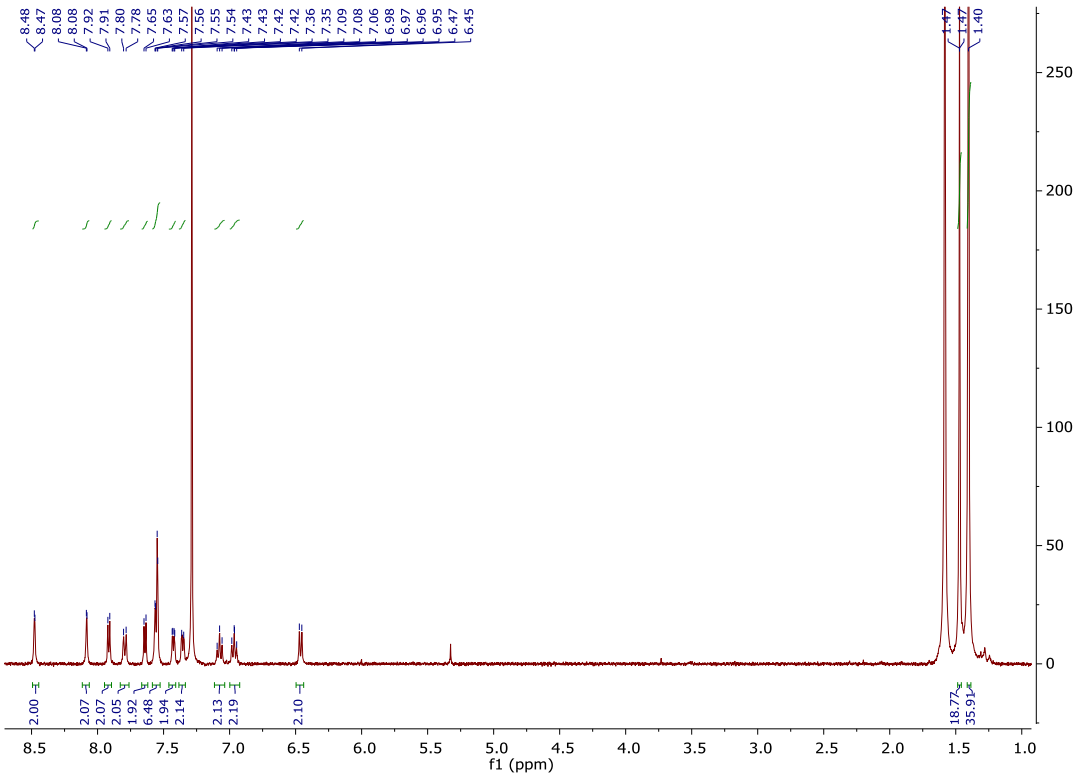

Figure **S22**. ^{1}H NMR spectra of **3a** in $CDCl_3$

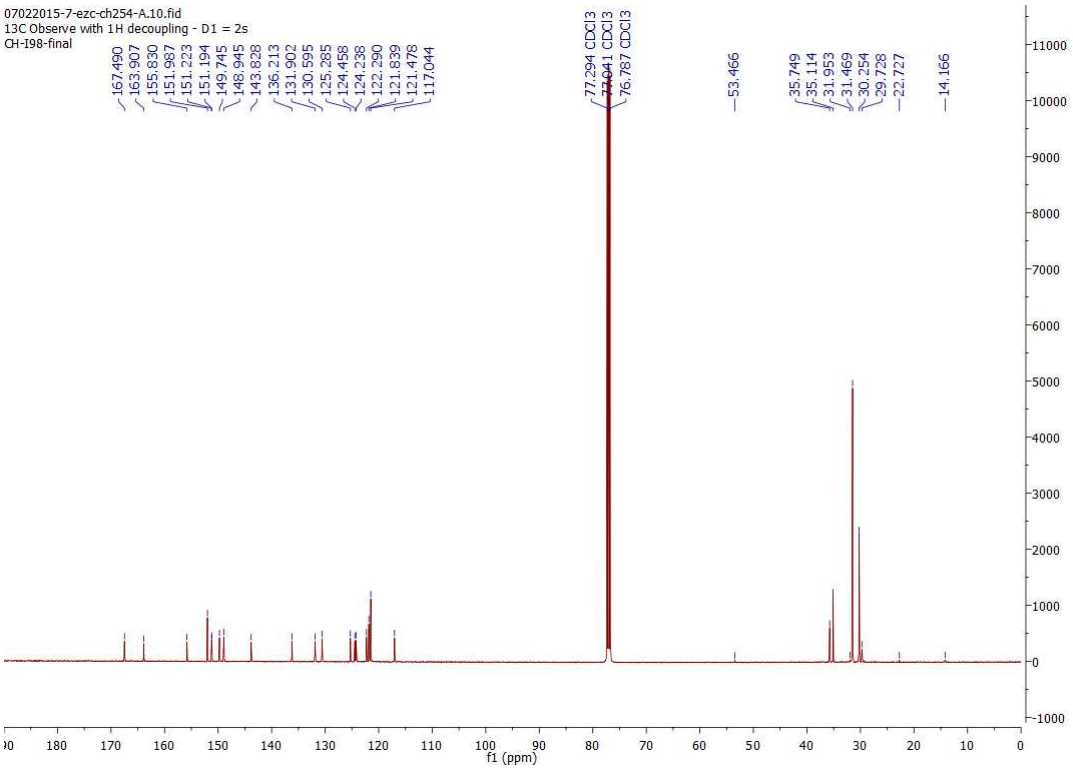

Figure **S23**. ^{13}C NMR spectra of **3a** in $CDCl_3$

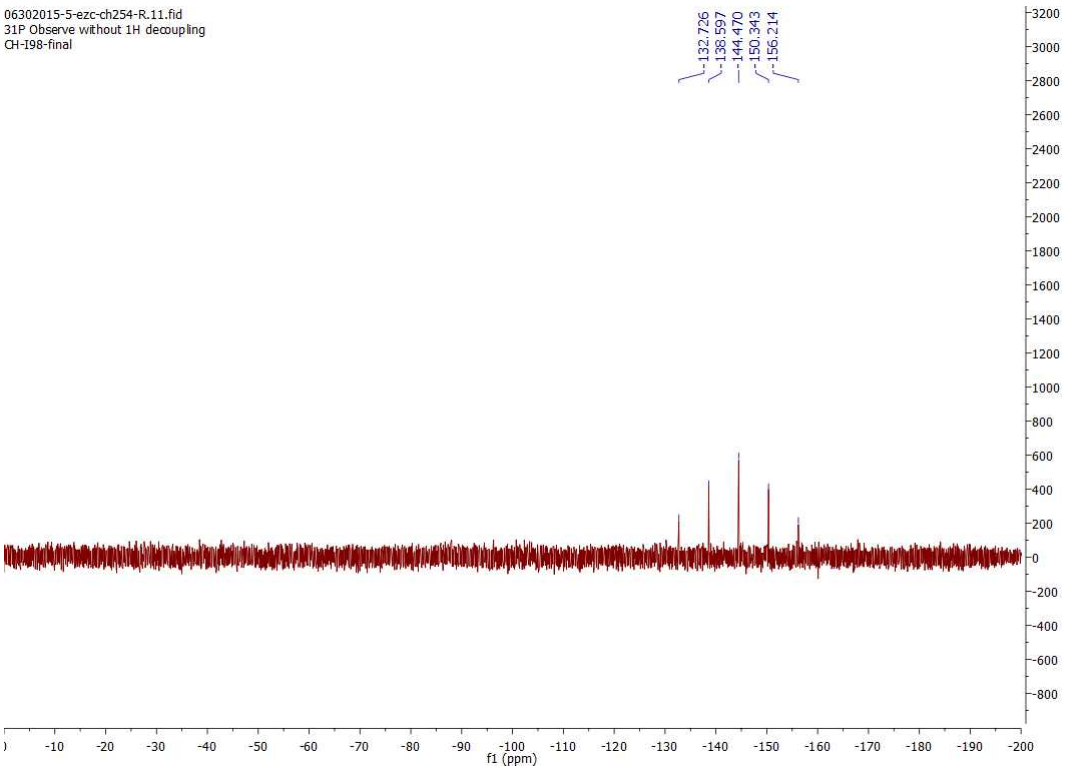

Figure **S24**. ^{31}P NMR spectra of **3a** in $CDCl_3$

X-ray Diffraction Studies

Single crystals of sufficient quality of **1a, 1b, R2** and **2a** were grown in a solution of CH_2Cl_2/Et_2O at -18 °C. The crystallographic data for **1a** and **2a** respectively at 140 K and 150 K were collected with an Oxford Diffraction Xcalibur3 diffractometer with a sealed monochromatic Mo-Kα radiation source (λ = 0.71073 Å). Xcalibur3 diffractometer was fitted with a Sapphire3 CCD detector and a nitrogen flow Oxford Cryosystems 700Plus series device. The crystallographic data for **1b** and **R2** at 140 K were collected with an Agilent Technology SuperNova diffractometer with a micro-focused monochromatic Cu-Kα radiation source (λ = 1.54184 Å). SuperNova diffractometer was fitted with an EosS2 CCD detector and a nitrogen flow Cryojet5 of Oxford Instruments with MercuryiTC controler.

Data collections, cell constants determination and data reduction were performed by using CrysAlisPro software (2014).[4] All structures were solved with the direct methods (Sir97) (Altomare et al., 1999)[5] and developed with the full least-squares refinement on F^2 (ShelxL) (Sheldrick, 2008, 2015).[6] Anisotropic displacement parameters were used for all non-hydrogen atoms. Hydrogen atoms were added at the calculated positions and refined using a riding model. Only for **1a** complex, ISOR restrain was applied in the refinement of the anisotropic displacement parameters for selected carbon, fluorine and phosphorus atom sites. Experimental details and structure determination parameters are given in Table **S1** and **S2**.

CCDC 1034962, 1038996, 1039805 and 1045877 respectively for **1a**, **1b**, **R2** and **2a** contain the supplementary crystallographic data for this paper. The data can be obtained free of charge from The Cambridge Crystallographic Data Centre via www.ccdc.cam.ac.uk/structures

Table **S1**. Crystallographic data for complexes **1a** and **1b**

	1a	**1b**
Empirical formula	C_{51} H_{62} Cl_6 F_6 Ir N_4 P	C_{60} H_{82} F_6 Ir N_4 O P
Crystal colour, shape	Yellow, prism	Yellow, prism
Crystal dimensions (mm^3)	0.232 x 0.184 x 0.143	0.225 x 0.052 x 0.038
Formula weight	1280.91	1212.46
Crystal system	Triclinic	Monoclinic
Space group	P-1	$P2_1$
a (Å)	14.5179(4)	10.71010(10)
b (Å)	14.7719(6)	20.1747(2)
c (Å)	15.0424(6)	14.31870(10)
α (°)	63.787(4)	90
β (°)	70.237(3)	108.5330(10)
γ (°)	87.517(2)	90
Volume ($Å^3$)	2702.2(2)	2933.44(5)
Z	2	2
ρ_{calcd} (g cm^{-3})	1.574	1.373
Temperature (K)	140(2)	140(2)
μ (mm^{-1})	2.856	5.162
θ range (°)	3.039 to 26.997	3.925 - 70.685
Ref. collected	20652	34539
Indep. Ref. (R_{int})	11770 (0.0285)	10848 (0.0507)
R_1 [I>2σ(I)]	0.0440	0.0391
wR_2 (all data)	0.1205	0.1087
Abs. stru. param.	n/a	-0.005(5)
Residual electron peak, hole (e.$Å^{-3}$)	1.348, -1.401	1.302, -1.281

Table **S2**. Crystallographic data for complexes **R2** and **2a**

	R2	**2a**
Empirical formula	C_{59} H_{62} Cl_2 F_6 Ir N_4 P	C_{59} H_{62} Cl_2 F_6 Ir N_4 O_2 P
Crystal colour, shape	Yellow, plate	Yellow, plate
Crystal dimensions (mm^3)	0.126 x 0.078 x 0.010	0.097 x 0.081 x 0.009
Formula weight	1235.19	1267.19
Crystal system	Monoclinic	Monoclinic
Space group	$P2_1$	$P2_1$
a (Å)	10.55450(10)	10.6303(2)
b (Å)	20.9658(3)	21.0524(5)
c (Å)	12.6119(2)	12.4988(3)
α (°)	90	90
β (°)	93.5550(10)	93.553(2)
γ (°)	90	90
Volume ($Å^3$)	2785.44(7)	2791.77(11)
Z	2	2
ρ_{calcd} (g cm^{-3})	1.473	1.507
Temperature (K)	140(2)	150(2)
μ (mm^{-1})	6.303	2.582
θ range (°)	3.511 - 70.603	3.116 - 26.997
Ref. collected	31112	21299
Indep. Ref. (R_{int})	8989 (0.0527)	10249 (0.0644)
R_1 [I>2σ(I)]	0.0356	0.0508
wR_2 (all data)	0.0908	0.1272
Abs. stru. param.	0.040(5)	-0.031(6)
Residual electron peak, hole (e.$Å^{-3}$)	1.379, -0.677	1.479, -1.068

LEEC preparation

All materials were used as received. Poly(3,4-ethylenedioxythiophene):poly-styrenesulfonate (PEDOT:PSS CLEVIOS™ P VP AI 4083) was purchased from Heraeus. The ionic liquid (IL) 1-butyl-3-methylimidazolium hexafluoridophosphate ([Bmim][PF_6]) and the solvent acetonitrile were purchased from Sigma-Aldrich. The photolithography-patterned indium tin oxide (ITO) glass substrates were purchased from Naranjo Substrates (www.naranjosubstrates.com).

The substrates were cleaned with sonication and soap, then deionized water, isopropanol, and UV−O_3 lamp for 20 min. The thickness of the films was determined with an Ambios XP-1 profilometer. 80 nm of (PEDOT:PSS) was coated at 1000 rpm for 60s then was dried at 150 ºC for 15 min. The emitting layer (100 nm) was prepared by spin-coating of a acetonitrile solution consisting of the Ir complex with the addition of the ionic liquid ([Bmim][PF_6]) in a 4:1 molar ratio. The devices were then transferred to an inert atmosphere glovebox (< 0.1 ppm O_2 and H_2O, MBraun) and annealed during 1 hour at 100 °C. Finally, a layer (70 nm) of aluminium (the top electrode) was thermally evaporated onto the devices using an Edwards Auto500 evaporator integrated in the inert atmosphere glovebox. The area of the device was 6.5 mm^2. The devices were not encapsulated and were characterized inside the glovebox at room temperature.

LEEC characterization: The device lifetime was measured by applying a pulsed current and monitoring the voltage and the luminance versus time by a True Colour Sensor MAZeT (MTCSiCT Sensor) with a Botest OLT OLED Lifetime-Test System. The average current density is determined by multiplying the peak current density by the time-on time and dividing by the total cycle time. The average luminance is directly obtained by taking the average of the obtained photodiode results and correlating it to the value of a luminance meter. The current efficiency is obtained by dividing the average luminance by the average current density. The

electroluminescent (EL) spectra were measured using an Avantes AvaSpec-2048 Fiber Optic Spectrometer during device lifetime measurement.

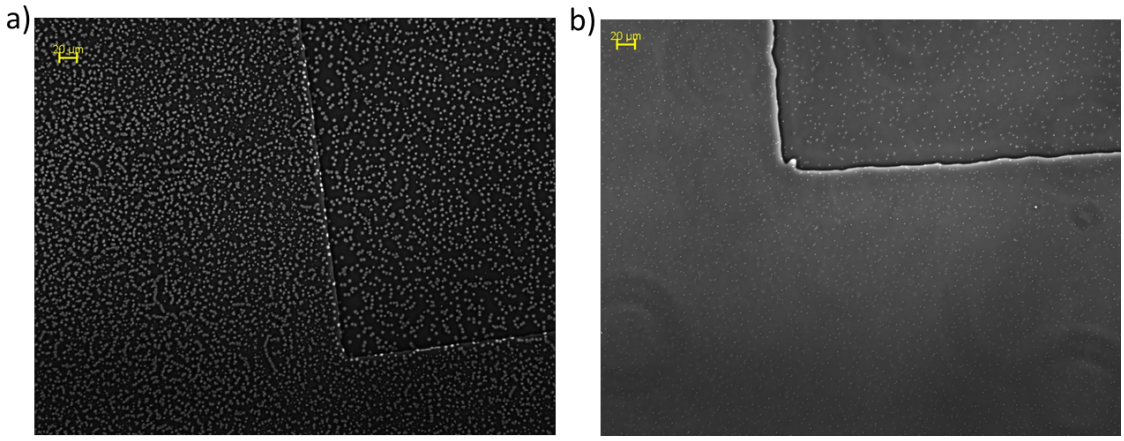

Figure **S25.** Optical microscope images of (a) D2a and (b) D3a. The areas on the top right corner are the patterned ITO. The images were recorded at 10x magnification. The scale is 20 µm.

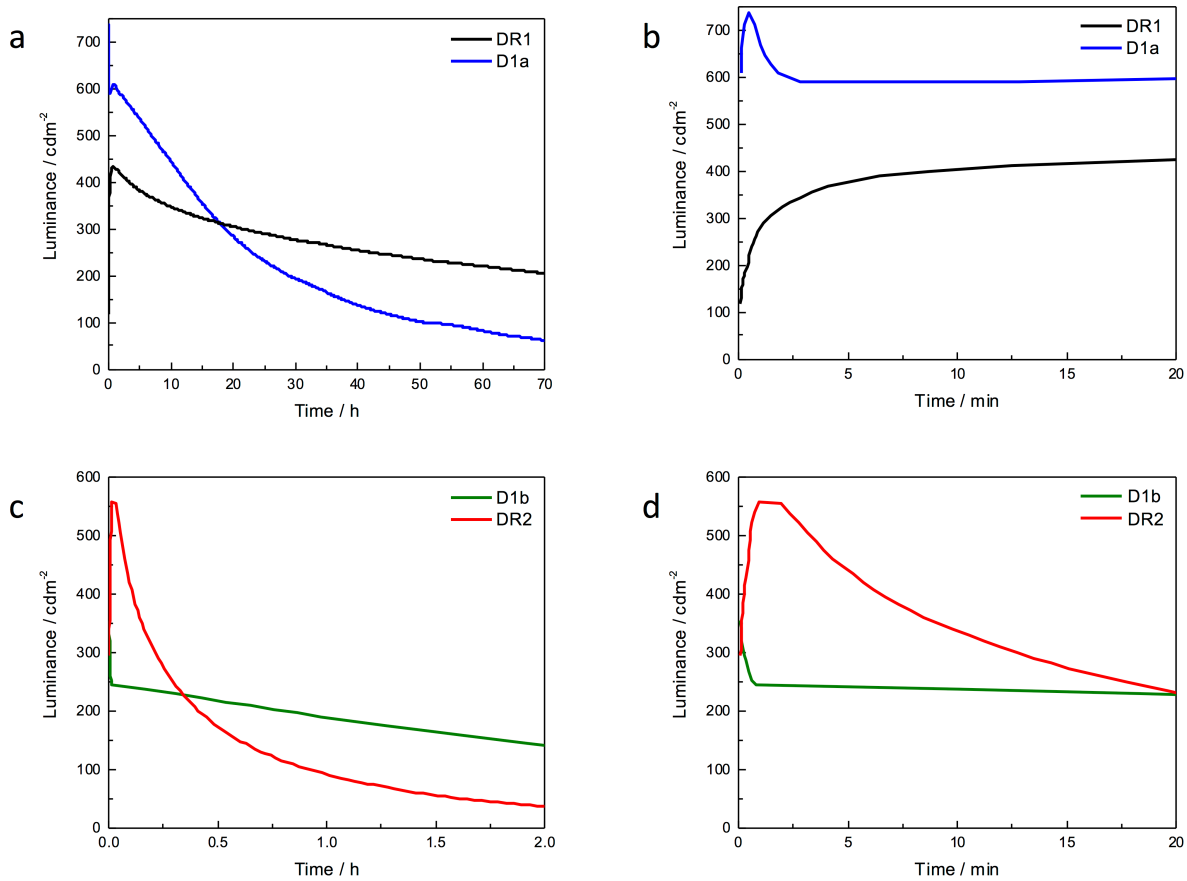

Figure **S26.** Luminance versus time (**DR1** and **D1a** in (a and b) and **D1b** and **DR2** in (c and d)) operated with a pulsed current of 100 A m^{-2} (1KHz, 50% duty cycle and block wave).

References

(1). V. V. Pavlishchuk and A. W. Addison, *Inorg. Chim. Acta*, 2000, **298**, 97-102.
(2). G. A. Crosby and J. N. Demas, *J. Phys. Chem.*, 1971, **75**, 991-1024.
(3). H. Ishida, S. Tobita, Y. Hasegawa, R. Katoh and K. Nozaki, *Coord. Chem. Rev.*, 2010, **254**, 2449-2458.
(4). *CrysAlisPro v1.171.37.34*, Agilent Technologies, 2014.
(5). A. Altomare, M. C. Burla, M. Camalli, G. L. Cascarano, C. Giacovazzo, A. Guagliardi, A. G. G. Moliterni, G. Polidori and R. Spagna, *J. Appl. Crystallogr.*, 1999, **32**, 115-119.
(6). (a) G. Sheldrick, *Acta Crystallogr., Sect. A*, 2008, **64**, 112-122; (b) G. Sheldrick, *Acta Crystallogr., Sect. A*, 2015, **71**, 3-8.